N92-28032

CALIBRATION OF A POLARIMETRIC IMAGING SAR

K. Sarabandi, L.E. Pierce, and F.T. Ulaby
Radiation Laboratory
Department of Electrical Engineering and Computer Science
The University of Michigan – Ann Arbor

Abstract

Calibration of polarimetric imaging SARs using point calibration targets is discussed. The four-port network calibration technique [5] is used to describe the radar error model. The polarimetric ambiguity function of the SAR is then found using a single point target, namely a trihedral corner reflector. Based on this, an estimate for the backscattering coefficient of the terrain is found by a deconvolution process.

A radar image taken by the JPL aircraft SAR is used for verification of the deconvolution calibration method. The calibrated responses of point targets in the image are compared both with theory and the POLCAL technique [8]. Also, responses of a distributed target are compared using the deconvolution and POLCAL techniques.

1 Introduction

Calibration techniques available in the literature can be categorized into two major groups: 1) calibration techniques for imaging radars, and 2) calibration techniques for point-target measurement systems, which may also be appropriate for imaging radars. In the first group, the scattering properties of clutter are usually employed to simplify the calibration problem such as in Sheen and Kasischke [1989], van Zyl [1990], and Klein [1989]. Among the point-target calibration techniques, are Whitt, et al. [1990], Barnes [1986], and Sarabandi, et al. [1990] which uses a sphere and any other depolarizing calibration target. However, the isolated antenna assumption can lead to significant errors when the ratio of cross- to like-polarized terms is small and/or cross-talk contamination is large. To remove this drawback, the single target calibration technique (STCT) has recently been developed [Sarabandi and Ulaby, 1990].

The main thrust of this paper is to show how the point target calibration techniques can be applied to imaging SARs. In particular, the STCT will be employed here since it only requires one calibration target. This method is then compared with the POLCAL technique [8] which has been developed specifically for imaging radars.

2 A New Approach for Calibration of Imaging SARs

In this new method the polarimetric ambiguity function of the SAR processor as well as the distortion matrices of the radar system are found from a trihedral corner reflector response. First a summary of the single target calibration technique (STCT) is given and then a theoretical model which relates the point target response to distributed targets will be developed. The model in conjunction with the STCT is then used to obtain a deconvolution matrix for estimation of the backscattering coefficient.

2.1 Single Target Calibration Technique

In this technique the antenna system and two orthogonal directions in free space are modeled as a four-port passive device. The measured scattering matrix of a target with real scattering matrix **s** is approximated by

$$\mathbf{U} = \begin{bmatrix} R_v & CR_v \\ CR_h & R_h \end{bmatrix} \mathbf{s} \begin{bmatrix} T_v & CT_h \\ CT_v & T_h \end{bmatrix}. \tag{1}$$

The complex quantities R_p, T_q are the receive and transmit channel distortions with $p, q = v, h$ and C is the antenna cross-talk factor. Once the distortion parameters of the radar system are found through the measurement of a trihedral corner reflector, $\mathbf{U}_t$, with radar cross section σ_t whose scattering matrix is diagonal, the actual scattering matrix of the target can be obtained from

$$\mathbf{s} = \frac{1}{R_v T_v (1+C^2)^2} \begin{bmatrix} 1 & -C\frac{R_v}{R_h} \\ -C & \frac{R_v}{R_h} \end{bmatrix} \mathbf{U} \begin{bmatrix} 1 & -C \\ -C\frac{T_v}{T_h} & \frac{T_v}{T_h} \end{bmatrix}. \tag{2}$$

with

$$C = \pm \frac{1}{\sqrt{a}} (1 - \sqrt{1-a}) \tag{3}$$

where the branch cut for $\sqrt{1-a}$ is chosen such that $\mathrm{Re}[\sqrt{1-a}] > 0$, and

$$a \triangleq \frac{u^t_{vh} u^t_{hv}}{u^t_{vv} u^t_{hh}}, \qquad R_v T_v = \frac{u^t_{vv}}{(1+C^2)\sqrt{\sigma_t / 4\pi}}, \tag{4}$$

$$\frac{R_v}{R_h} = \frac{1+C^2}{2C} \cdot \frac{u^t_{vh}}{u^t_{hh}}, \qquad \frac{T_v}{T_h} = \frac{2C}{1+C^2} \cdot \frac{u^t_{vv}}{u^t_{vh}}. \tag{5}$$

The single target calibration technique (STCT) has been tested both under laboratory and field conditions using L-, C-, and X-band scatterometer systems and it has been shown that a calibration accuracy of 0.5 dB in amplitude and 5 degrees in phase can be achieved.

2.2 Difficulties in Calibration of SARs Using Point Targets

To understand the steps involved in calibration of imaging SARs using point calibration targets, the generation of a high resolution image from raw data must be examined. The received raw data in each of the channels of a polarimetric SAR can be described by

$$U_{pq}(t) = \int_A S^0_{pq}(x', y') \, f\left(t - \frac{2R}{c}\right) dx' dy' \quad p, q = v, h \tag{6}$$

where A is the illumination area by the physical antenna, $S^0_{pq}(x', y')$ is the reflectivity of the terrain being mapped ($\sigma^0_{pq}(x, y) = 4\pi \mid S^0_{pq}(x, y) \mid^2$), and p and q are the polarization state of the receiver and transmitter respectively. Function $f(t)$ is a particular wave form radiated by the transmitter and can usually be represented by

$$f(t) = g(t) \, e^{i\omega_0 t} \tag{7}$$

where $g(t)$ is a slowly varying function and ω_0 is the angular frequency of the radar system. In equation (6) R is the distance from the antenna to the scattering point (x', y') on the ground.

One way to retrieve the backscattering coefficient $\sigma^0_{pq}(x,y)$ from the received signal $U_{pq}(t)$ is to pass the signal through a matched filter having an impulse response $f^*\left(t - \frac{2R}{c}\right)$ [Cutiona, 1970], that is

$$U'_{pq}(x,y) = \int_t \int_A \sigma^0_{pq}(x',y') f\left(t - \frac{2R'}{c}\right) f^*\left(t - \frac{2R}{c}\right) dx'dy'dt \tag{8}$$

By performing the integration with respect to time, the quantity

$$\psi(x,y;x',y') = \int_t f\left(t - \frac{2R'}{c}\right) f^*\left(f - \frac{2R}{c}\right) dt \tag{9}$$

known as the ambiguity function can be obtained. Therefore (8) can be written as

$$U'_{pq}(x,y) = \int_A \sigma^0_{pq}(x',y')\,\psi(x,y;x',y')\,dx'dy' \ . \tag{10}$$

If the ambiguity function is a Dirac delta function, i.e. $\psi(x,y;x',y') = \delta(x-x', y-y')$, the backscattering coefficient can be directly obtained from (10).

By substituting (7) into (9) and assuming that $g(t)$ is a linearly frequency-modulated pulse of duration τ $\left(g(t) = e^{i\frac{\pi\Delta f}{\tau}t^2}\right)$ and that the integration time in (9) is over $N+1$ pulses of the transmitter we have

$$\psi(x,y;x',y') = \sum_{-\frac{N}{2}}^{\frac{N}{2}} e^{-2iw_0(R-R')/c} \int_{-\tau/2}^{\tau/2} e^{i\frac{\pi\Delta f}{\tau}\left[\left(t-\frac{2R'}{c}\right)^2 - \left(t-\frac{2R}{c}\right)^2\right]} dt \tag{11}$$

Using (11) in (10) does not resolve $\sigma^0_{pq}(x,y)$ completely. To obtain a better estimate a deconvolution process must be attempted. This requires that the calibration technique be able to estimate the ambiguity function.

2.3 Calibration Procedure and Estimation of Backscattering Coefficient

The error model for a polarimetric SAR must include the uncertainties such as the antenna cross talk and channel imbalances as well as the uncertainties in the ambiguity function. Suppose the radar system is linear. The polarimetric response of the terrain with polarimetric reflectivity $\mathbf{S}^0(x,y)$ is given by

$$\mathbf{U}(x,y) = \mathbf{R}\left[\int_A \mathbf{S}^0(x',y')\,\psi(x,y;x',y')dx'dy'\right]\mathbf{T} \ . \tag{12}$$

In (12) the amplitude and phase of the propagation factor $\left(\frac{e^{2ik_0R}}{R^2}\right)$ has been excluded and $\mathbf{R}$ and $\mathbf{T}$ are, respectively, the receive and transmit distortion matrices. Assume

$\psi(x,y;x',y') = \psi(x-x',y-y')$. Since radar images are discretized into a finite number of pixels, the discretized form of (12) must be considered, where the integral is approximated by a double summation, thus

$$\mathbf{U}(m,n) = \mathbf{R}\left[\sum_i \sum_j \mathbf{S}^0(i,j)\psi(m-i,n-j)\,\Delta x \Delta y\right]\mathbf{T} \tag{13}$$

By changing the index of the summations such that the maximum of the ambiguity function occurs at $(0,0)$, and lumping together the ambiguity function and distortion matrices, equation (13) becomes

$$\mathbf{U}(m,n) = \Delta x \Delta y \sum_{i=\frac{-N}{2}}^{\frac{N}{2}} \sum_{j=\frac{-M}{2}}^{\frac{M}{2}} \mathbf{AR}_{ij}\,\mathbf{S}^0(m-i,n-j)\;\mathbf{AT}_{ij} \tag{14}$$

where $\mathbf{AR}_{ij}$ and $\mathbf{AT}_{ij}$ are the receive and transmit ambiguity-distortion matrices respectively.

If a trihedral with radar cross section σ_T located at (x_0,y_0) is used as a calibration target, its reflectivity function is expressed by

$$\mathbf{S}_T^0(x,y) = \sqrt{\frac{\sigma_T}{4\pi}}\quad \mathbf{I}\quad \delta(x-x_0)\,\delta(y-y_0) \tag{15}$$

where $\mathbf{I}$ is a 2×2 identity matrix. Substituting (15) into (12) results in the polarimetric response of the SAR to the trihedral. When the discretized form of this response is combined with the resultant ambiguity function and distortion matrices, the response becomes

$$\mathbf{U}_T(k+i,l+j) = \sqrt{\frac{\sigma_T}{4\pi}}\;\mathbf{AR}_{ij}\;\mathbf{I}\;\mathbf{AT}_{ij} \tag{16}$$

with

$$i \in \left\{-\frac{N}{2},\cdots,\frac{N}{2}\right\} \text{ and } j \in \left\{-\frac{M}{2},\cdots,\frac{M}{2}\right\}\ ,$$

where $i = m-k$ and $j = n-l$ for a trihedral at the klth pixel. Figure (1) shows the measured amplitude of the polarimetric response of the JPL aircraft SAR to an 8-foot trihedral.

An approximate form of (14) can be obtained by assuming that over the pixels where the ambiguity function is non-zero the reflectivity of the terrain is constant and is equal to that of the center pixel, giving

$$\mathbf{U}(m,n) = \Delta x \Delta y \sum_{i=\frac{-N}{2}}^{\frac{N}{2}} \sum_{j=\frac{-M}{2}}^{\frac{M}{2}} \mathbf{AR}_{ij}\,\hat{\mathbf{S}}^0(m,n)\;\mathbf{AT}_{ij} \tag{17}$$

If the four-vector form of $\mathbf{U}(m,n)$ and $\hat{\mathbf{S}}^0(m,n)$ are, respectively, denoted by

$$\mathcal{U}(m,n) = \begin{bmatrix} U_{vv}(m,n) \\ U_{vh}(m,n) \\ U_{hv}(m,n) \\ U_{hh}(m,n) \end{bmatrix}, \quad \hat{\mathcal{S}}^0(m,n) = \begin{bmatrix} \hat{S}^0_{vv}(m,n) \\ \hat{S}^0_{vh}(m,n) \\ \hat{S}^0_{hv}(m,n) \\ \hat{S}^0_{hh}(m,n) \end{bmatrix}$$

then (17) becomes

$$\mathcal{U}(m,n) = \left[\sum_{i=\frac{-N}{2}}^{\frac{N}{2}} \sum_{j=\frac{-M}{2}}^{\frac{M}{2}} \mathbf{D}_{ij} \right] \hat{\mathcal{S}}^0(m,n) \triangleq \mathbf{D}\hat{\mathcal{S}}^0(m,n) \ . \tag{18}$$

where $\mathbf{D}$ is the deconvolution matrix which is independent of pixel coordinates m and n. Therefore the calibrated estimate of the reflectivity matrix is given by

$$\hat{\mathcal{S}}^0(m,n) = \mathbf{D}^{-1}\,\mathcal{U}(m,n) \ .$$

3 JPL POLCAL Technique

POLCAL [van Zyl et al., 1990] is a combination of phase calibration by Zebker and Lou [1990] and a calibration algorithm by van Zyl [1990] based on properties of distributed targets. In this technique the radar error model and corrections are done in three steps. The first step is phase calibration where the radar distortion matrices are assumed to be diagonal with only phase differences. That is, the measured scattering matrix is assumed to be

$$\mathbf{U} = \begin{bmatrix} s_{vv} & s_{vh}e^{i\phi_r} \\ s_{hv}e^{i\phi_t} & s_{hh}e^{i(\phi_r+\phi_t)} \end{bmatrix}.$$

where s_{pq} are the theoretical values for the scattering matrix elements. Reciprocity mandates that $s_{hv} = s_{vh}$ and therefore the quantity $u_{hv}u_{vh}^*$ must have zero phase. The phase difference $\phi_t - \phi_r$ is averaged over the entire image, then subtracted from u_{hv}, to form a matrix $\mathbf{Z}$ whose off-diagonal elements have almost identical phases. Next this matrix is symmetrized by averaging the off-diagonal elements and then stored in the matrix $\mathbf{Y}$. The data is then coded and stored in the form of the Stokes scattering operator, with groups of four adjacent pixels in a row being summed. The quantity $\phi_r + \phi_t$ is obtained from a trihedral response by calculating $Y_{hh}Y_{vv}^*$.

The next steps include cross-talk removal and adjusting for co-channel gain balance. Here the radar error model of the phase calibrated symmetrized response ($\mathbf{Y}'$) is represented by reciprocal transmit and receive distortion matrices, i.e.

$$\mathbf{Y}' = A \begin{bmatrix} 1 & \delta_2 \\ \delta_1 & f \end{bmatrix} \mathbf{s} \begin{bmatrix} 1 & \delta_1 \\ \delta_2 & f \end{bmatrix}. \tag{19}$$

where $\mathbf{s}$ is the actual scattering matrix of the target, δ_1 and δ_2 represent the antenna cross-talk, and f is the co-channel imbalance. Using the above equations δ_1 and δ_2/f are found iteratively. The amplitude of the co-channel imbalance f is obtained by calculating the ratio of the total power of VV to HH of a corner reflector response over 16×16 surrounding pixels. However, it is left unjustified why the HH and VV responses should be added noncoherently.

4 Results and Comparison

This section presents the results of applying the three different calibration techniques described in sections 2.1, 2.3, and 3 to the same scene. Each technique was applied twice,

each time with a different calibration target, which helped in determining the reproducibility of the calibration.

4.1 Data Formats and Test Scene

The results given in this section were obtained by processing the same JPL AirSAR scene as provided by JPL in two different formats. The format used by the techniques described in section 2 is the so-called "hires" format, which provides the four scattering matrix elements as single-precision (4-byte) complex numbers. The format used by the POLCAL technique is radically different. The symmetrization, quantization from 4 bytes to 1, and summing from 1-look to 4-look, as described in section 3, have been carried out to produce the so-called "compressed" format.

Figure 2 shows the total power image of the particular scene used during this study. Figure 3 shows the uncalibrated HH polarized raw data in the vicinity of the three trihedrals. Note that the trihedrals are identical but that the responses are not, which is of great concern when calibration depends on identical responses to identical targets. Also, a distributed target, as outlined in Fig. 2, was used for comparisons despite the lack of any known values for its cross sections.

4.2 Assessment of STCT

Figure 4 shows the calibrated polarization signatures for the trihedral that was **not** used as calibration target, in each of the two cases. The results are excellent: the levels are within 1 dB of theory, with the co-channel imbalance no more than 0.5 dB. Also, the cross-to-like isolation has improved from 20 dB before calibration to about 40 dB.

Figure 5 shows the calibrated signatures of two different PARCs: VV and 45°. The VV PARC signature is as expected with a 23 dB isolation between VV and HH. The 45° PARC signature has the peak very nearly centered on $\chi = 0, \Psi = 45°$, as expected. Because of this favorable comparison with the expected results one can conclude that this technique is applicable to the JPL AirSAR imaging radar data.

4.3 Assesment of POLCAL

Because the calibration trihedral is used only to determine the co-channel imbalance and absolute level, this calibration technique gives noticeably different results when compared to those in section 4.2. Figure 6 shows the single-pixel signatures of various trihedrals after calibration with POLCAL. Here the co-channel imbalance is between 0.5 dB and 1 dB, slightly worse than for STCT. The cross-to-like isolation is generally 23 dB, 17 dB worse than for STCT, while one has an isolation of 175 dB, apparently a fluke since it appears only once.

To compare the absolute levels, the signatures are computed by summing over the same region that is used to sum the powers of the calibration target. These results are shown in Fig. 7. Generally the signatures do not as closely resemble a trihedral as did those when using just a single pixel (Fig. 6). The absolute levels, however, are within 1 dB of the expected levels.

Figure 8 shows the same two PARCs as before, however they look quite different using

the POLCAL calibration scheme. The VV PARC has a 15 dB isolation, 8 dB worse than STCT, while the cross-pol signature is significantly distorted due to the symmetrization step: the 45° PARC now has **two** cross-pol peaks, at ±45°.

4.4 Comparison using a distributed target

First, a comparison of the two formats, uncalibrated, is in order. Figure 9 shows that the hires data has a VV power of about 3.75 dB less than HH, while the compressed data has them 4.75 dB apart. There are similar differences after calibration as well.

The deconvolution calibration scheme described in Sec. 2.3 was used, with the summation on $\mathbf{D}_{ij}$ done over all pixels in the vicinity of the calibration target that had a cross-pol magnitude about 20 dB above the noise. The results are shown in Fig. 10. The signatures are very similar, the only difference being in their absolute levels – a difference of at most 0.75 dB. Hence, the differences in the measured ambiguity function for the different calibration targets do not significantly affect the calibration of distributed targets. Figure 11 shows the results of the POLCAL calibration and looks very similar to the results in Fig. 10. The difference between the two calibration schemes is only on the order of 1 dB.

5 Conclusions

A new method for calibration of polarimetric imaging SARs using point targets has been developed. The technique requires a single calibration target, namely a trihedral, to find the ambiguity-distortion matrix (polarimetric ambiguity) function of the SAR system.

The validity of the technique is examined by calibrating a scene which includes a variety of point targets with known scattering matrices. It is found that the error model provided by STCT is an appropriate one and enhances the measured polarization of the point targets. The deconvolution technique compares favorably with the POLCAL technique for absolute radiometric calibration of distributed targets. This new technique is preferred to POLCAL only if the radar system has large distortions.

Acknowledgement

This project was conducted under JPL contract #JPL-C-958749. The authors appreciate the help of the JPL Radar Science group in providing the POLCAL software and the AirSAR image data used here.

References

[1] Barnes, R.M., "Polarimetric calibration using in-scene reflectors," Rep. TT.65, MIT, Lincoln Laboratory, Lexington, MA, Sept. 1986.

[2] Cutrona, L. J., "Synthetic aperture radar," Radar Handbook, (Ed. M. Skolnik), McGraw-Hill, 1970.

[3] Klein, J. D.,"Calibration of quadpolarization SAR data using backscattering statistics," Proc. 1989 Intern. Geosci. Remote Sens. Symp., Vancouver, Canada, July 1989.

[4] Sarabandi, K., F.T. Ulaby, and M.A. Tassoudji, "Calibration of polarimetric radar systems with good polarization isolation," *IEEE Trans. Geosci. and Remote Sens.*, vol. 28, no. 1, Jan. 1990.

[5] Sarabandi, K., and F.T. Ulaby, "A Convenient technique for polarimetric calibration of single-antenna radar systems," *IEEE Trans. Geosci. and Remote Sens.*, vol. 28, no. 6, Nov. 1990.

[6] Sheen, D.R. and E.S. Kasischke,"Comparison of SAR polarimetric calibration technique using clutter," Proc. 1989 Intern. Geosci. Remote Sens. Symp., Vancouver, Canada, July 1989.

[7] Ulaby, F.T., and Elachi C., eds. Radar Polarimetry for Geoscience Applications, Artech, 1990.

[8] van Zyl, J. J., " Calibration of polarimetric radar images using only image parameters and trihedral corner reflector responses," *IEEE Trans. Geosci. and Remote Sens.*, vol. 28, no. 3, May 1990.

[9] van Zyl, J. J., C.F. Burnette, H. A. Zebker, A. Freeman, and J. Holt, "POLCAL User's Manual," Jet Propulsion Laboratory, D-7715, Aug. 1990.

[10] Whitt, M.W., F.T. Ulaby, P. Polatin, and V.V. Liepa, "A general polarimetric radar calibration technique," *IEEE Trans. Antennas Propagat.*, vol. 39, no. 1, Jan. 1991.

[11] Zebker, H. A., and Y. Lou, "Phase calibration of imaging radar polarimeter Stokes matrices," *IEEE Trans. Geosci. and Remote Sens.*, vol. 28, no. 2, March 1990.

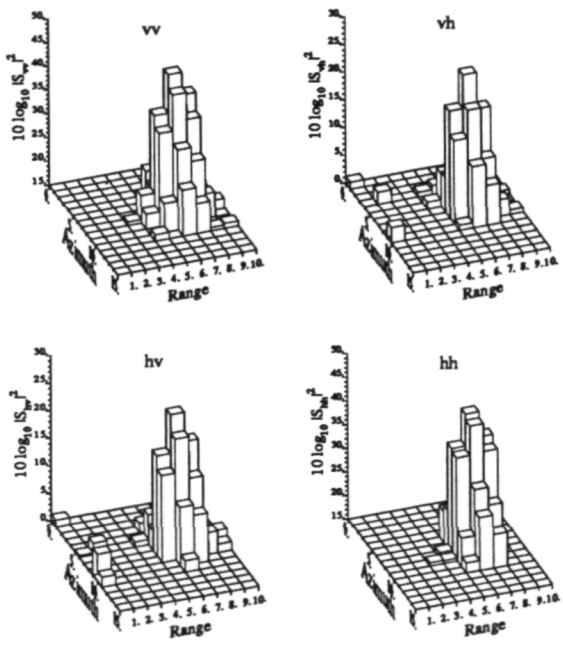

Figure 1: Measured Ambiguity-Distortion Matrix values in dB for a single trihedral. A small region surrounding the brightest pixel is shown.

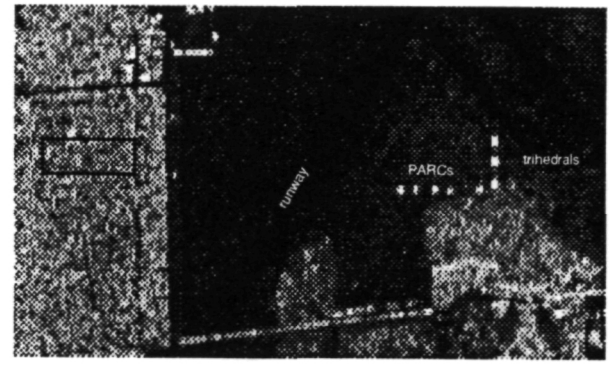

Figure 2: Total Power image of calibration targets and surrounding area. Shown are all three trihedrals, the five PARCs, and the distributed target area to the left.

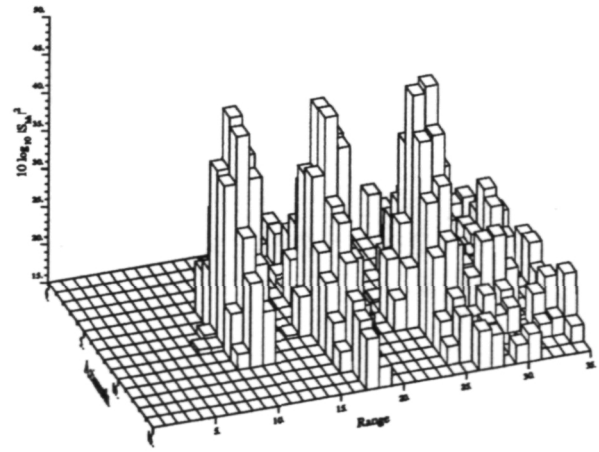

Figure 3: Measured HH-polarized values in dB for all three trihedrals. A small region surrounding them is shown. Note that the response is significantly different for the identical trihedrals.

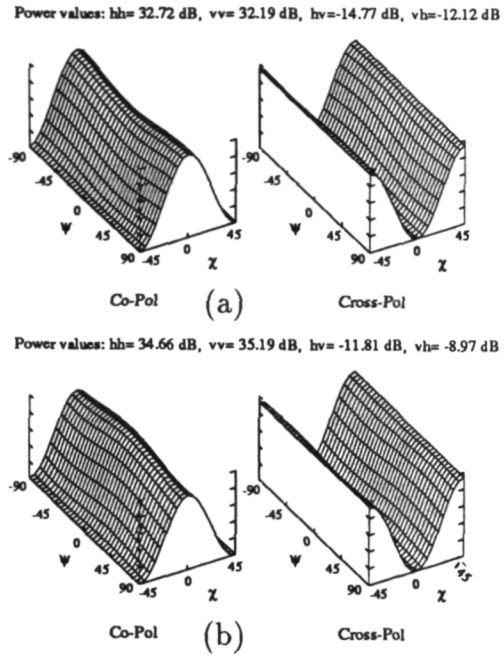

Figure 4: Validation results for STCT. (a) shows trihedral #2 when the calibration target was trihedral #1. (b) shows trihedral #1 when the calibration target was trihedral #2.

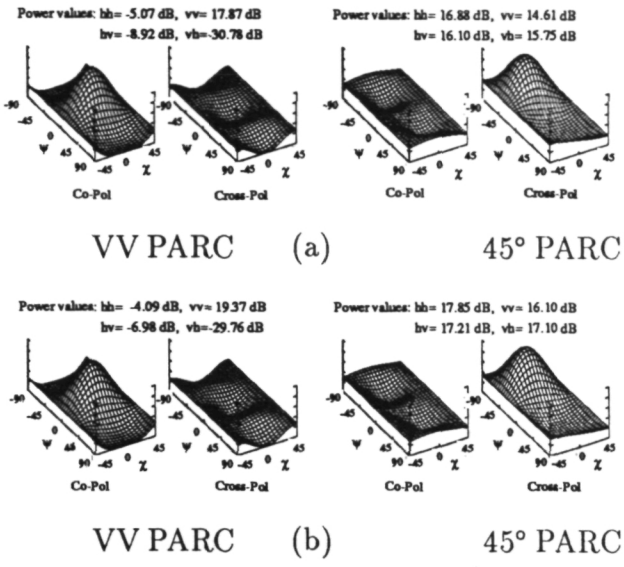

Figure 5: Validation results for STCT. (a) shows the VV and 45° PARCs when the calibration target was trihedral #1. (b) shows the VV and 45° PARCs when the calibration target was trihedral #2.

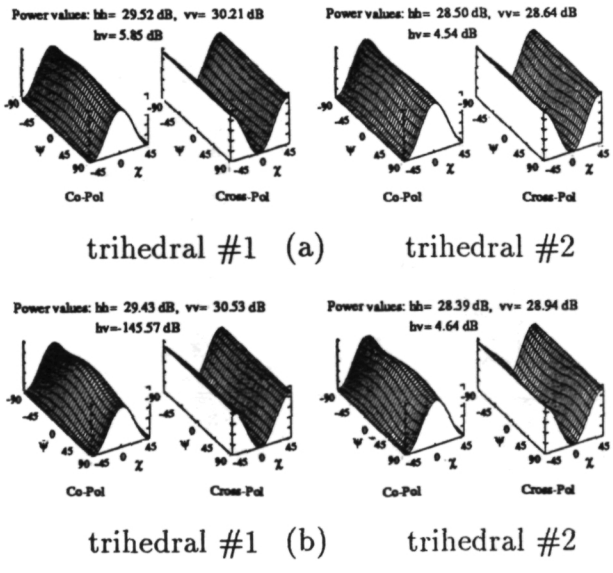

Figure 6: Validation results for POLCAL, displaying only 1 pixel. (a) shows both trihedrals when the calibration target was trihedral #1. (b) shows both trihedrals when the calibration target was trihedral #2.

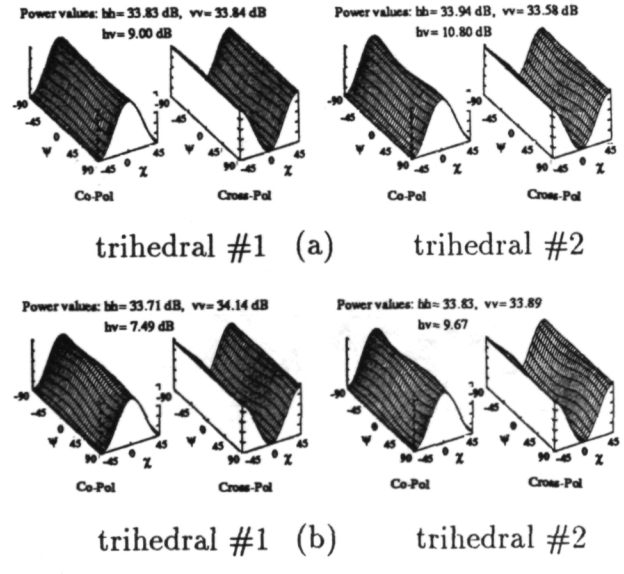

Figure 7: Validation results for POLCAL, displaying sum over adjacent area. (a) shows both trihedrals when the calibration target was trihedral #1. (b) shows both trihedrals when the calibration target was trihedral #2.

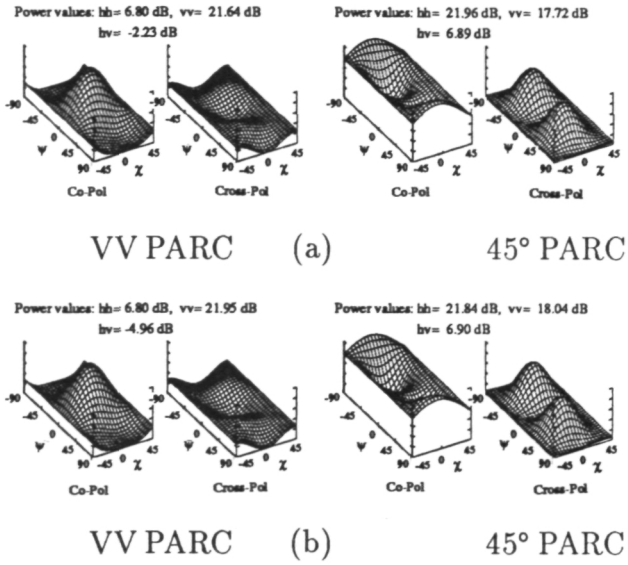

Figure 8: Validation results for POLCAL, displaying only 1 pixel. (a) shows the VV and 45° PARCs when the calibration target was trihedral #1. (b) shows the VV and 45° PARCs when the calibration target was trihedral #2.

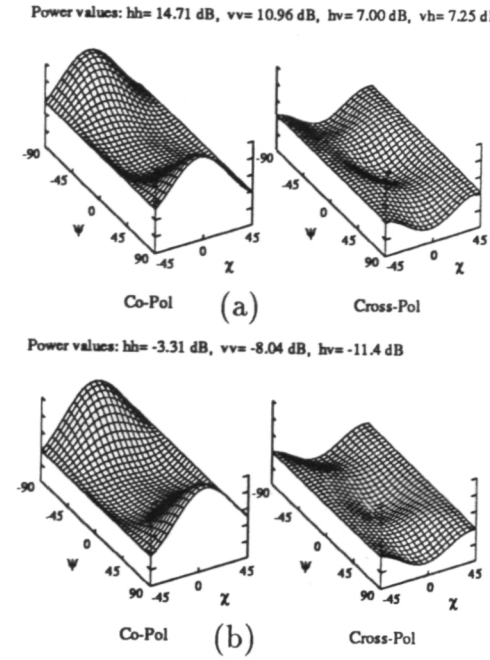

Figure 9: Uncalibrated Signature of distributed target region. (a) shows the hires format, (b) shows the compressed format.

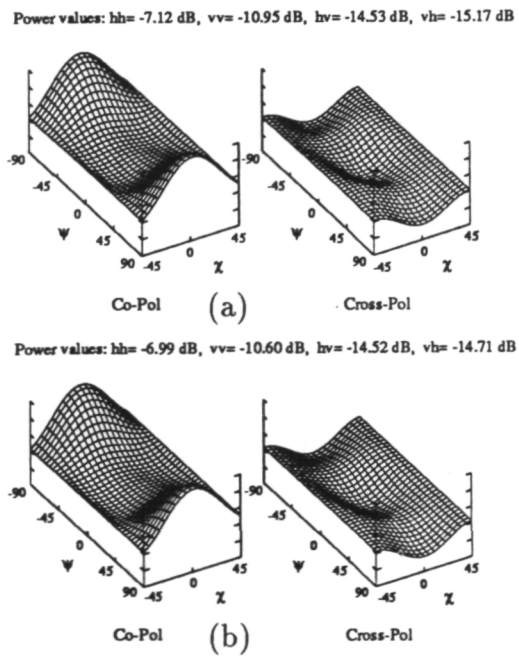

Figure 10: Signature of distributed target region, Deconvolution calibration. (a) shows the response with trihedral #1 as the calibration target. (a) shows the response with trihedral #2 as the calibration target.

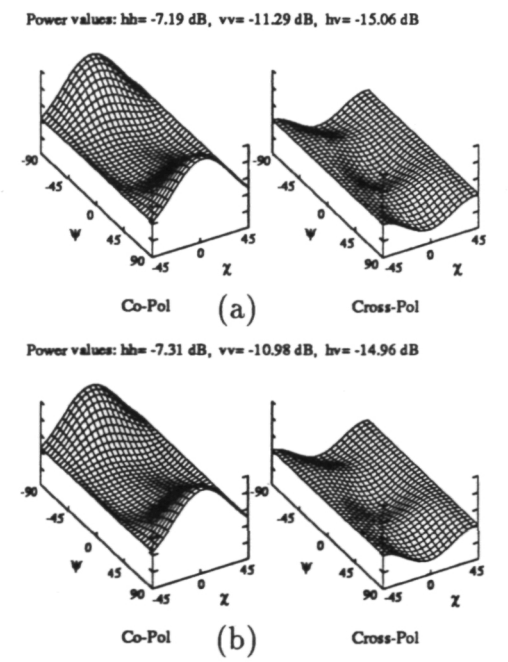

Figure 11: Signature of distributed target region, POLCAL calibration. (a) shows the response with trihedral #1 as the calibration target. (a) shows the response with trihedral #2 as the calibration target.